ISSN: 2230-9926

Available online at http://www.journalijdr.com

IJDR

International Journal of Development Research
Vol. 12, Issue, 05, pp. 55994-56004, May, 2022
https://doi.org/10.37118/ijdr.24579.05.2022

RESEARCH ARTICLE OPEN ACCESS

EXERGOECONOMIC ANALYSIS OF A MUNICIPAL SOLID WASTE FIRED POWER PLANT WITH BIOLOGICAL FILTERS FOR EMISSIONS

Renan Manozzo Galante[1,6,8,*], José Viriato Coelho Vargas[1,2,3,6], Lúcio Cardozo-Filho[4], André Bellin Mariano[2,5], Wellington Balmant[1,6], Guilherme de Paula Prado[8] and Vanessa Merlo Kava[6,7]

[1]Programa de Pós-Graduação em Engenharia Mecânica, Universidade Federal do Paraná, Curitiba, PR, 81531-980, Brazil; [2]Programa de Pós-Graduação em Engenharia e Ciência dos Materiais, Universidade Federal do Paraná, Curitiba, PR 81531-980 Brazil; [3]Departamento de Engenharia Mecânica, Universidade Federal do Paraná, Curitiba, PR, 81531-980, Brazil; [4]Departamento de Engenharia Química, Universidade Estadual de Maringá, Maringá, PR, 87020-900, Brazil; [5]Departamento de Engenharia Elétrica, Universidade Federal do Paraná, Curitiba, PR, 81531-980, Brazil; [6]Núcleo de Pesquisa e Desenvolvimento em Energia Auto–Sustentável, Universidade Federal do Paraná, Curitiba, PR, 81531-980, Brazil; [7]Departamento de Genética, Programa de Pós-Graduação em Genética, Universidade Federal do Paraná, Curitiba, PR, 81531-980, Brazil; [8]Coordenação de Engenharia Mecânica, Universidade Tecnológica Federal do Paraná, Guarapuava, PR, 85053-525, Brazil

ARTICLE INFO

Article History:
Received 22nd February, 2022
Received in revised form
19th March, 2022
Accepted 27th April, 2022
Published online 20th May, 2022

Key Words:
Exergoeconomic Analysis, Municipal Solid Waste, Sustainable Energy, Photobioreactor.

****Corresponding author:***
Renan Manozzo Galante

ABSTRACT

In the last few decades, the energy demand has vastly increased, and the generation of municipal solid wastes (MSW) in the cities represents extraordinary challenges for sustainable economic growth. Aiming to mitigate these problems, this work verifies an MSW fired power plant's technical and economic viability that uses biological filters for carbon dioxide fixation and microalgae biomass production. An exergoeconomic analysis is undergone in a southern Brazil waste-to-energy (WtE) plant with an incineration capacity of 50 kg/h, providing hot flue gases for a set of heat exchangers that operate as the system boiler for a 15-kW water Rankine cycle. The system sums six 10 m³ tubular Photobioreactor (PBR) producing up to 30,000 kg/year of microalgae biomass with the southern Brazil solar conditions of 1.732 kWh/m² per year. Considering a payment for the incineration services, this integrated power plant could reach a payback as low as 3.39 years, with biomass costing as low as 0.39 US$/kg and emissions factor that could reach 22.3 g_{CO2}/kWh. Therefore, this system shows a capacity to produce clean electricity treating the MSW and provide microalgae biomass that can be processed into animal food and bio-fuels.

Citation: ***Renan Manozzo Galante, José Viriato Coelho Vargas, Lúcio Cardozo-Filho, André Bellin Mariano, Wellington Balmant, Guilherme de Paula Prado and Vanessa Merlo Kava.*** "Exergoeconomic analysis of a municipal solid waste fired power plant with biological filters for emissions", *International Journal of Development Research*, 12, (05), 55994-56004.

INTRODUCTION

The worldwide population distribution has changed in the last decades, reducing the low-density rural areas share compared to the high-density coastline cities. These urbanized areas are related to high consume rate of goods and fuels and related to great generation of municipal solid wastes (MSW). Even with the MSW correct destination in landfills, it will lead to a value decrease to the neighboring lands and methane emissions due to the biomass decomposition. The MSW incineration is an alternative to the landfills, reducing the volume of discarded materials up to 90% while supplying thermal energy to be used as heat or electricity generation (1). A better balance between the need for resources consumption and environment degradation could be aided by biofuels since they do not increase the net amount of CO_2 in the atmosphere while supplying energy to society. In this scenario, the microalgae could have a leading role, since its production do not compete with food prices, northe available arable land, and shows higher lipids content compared to the traditional crops. The content of oil in microalgae dry biomass can surpass 80%, with values from 20% to 50% been described as common results (2–5). The two most used methods for microalgae production are the raceways ponds and the photobioreactors. In both approaches it is possible to inject flue gas that comes from powerplants or internal

combustion engines to supply a higher amount of CO_2 to the microalgae while reducing the emissions to the atmosphere (6–10). Depending on the source of energy and conversion technology used, the power generation facilities achieve diverse ranges of emission of CO_2 per kWh of energy converted, known as Emission Factor (*EF*).

Values of *EF*varies from 660 to 1250 g_{CO2}/kWh for system running with coal, from 380 to 1000 g_{CO2}/kWh for natural gas, from 97 to 1000 g_{CO2}/kWh for waste-to-energy (WtE) and from 1 to 550 g_{CO2}/kWh for biomass, for several case of studies (11). This work analysis an MSW fired power plant with biological filters for the flue gas as an alternative to landfills. The MSW comes from a university campus, and in this stage, mostly biomass residues are used as fuel to verify the concept. The combustion rich CO_2 flue gas is supplied to the PBR set with a total volume of 60 m³. This facility is in the south of Brazil, in the city of Curitiba. Agro-industrial wastewater is digested for biogas production and its treated effluents are sent to a set of PBR to absorb the required nutrients to the microalgae growth. An exergoeconomic analysis, as described by Bejan *et al*. (12), is applied to the system described in Figure 1to investigate for technical and economic system viability while pursuing the optimization of individual components. It is also this work objective to verify the hypothesis of clean energy production with this integrated approach.

METHODS

The systemis shown in detail in the Figure 1, where is depicted the ventilation and incineration structure, the heat exchanger unit with boiler and preheaters, the Rankine cycle and the PBR units. Steady state is considered in the model developed with the software Engineering Equation Solver (EES) (13) which includes thermodynamic property libraries for the fluids used.

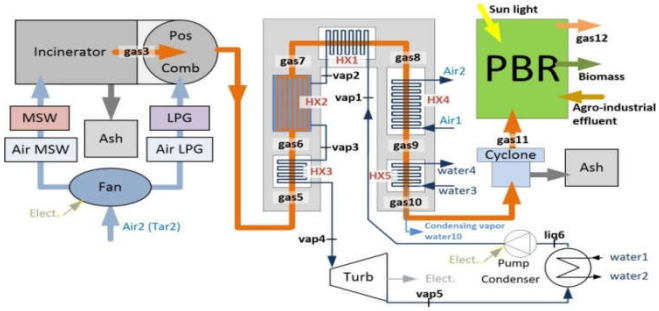

Figure 1. The connected incineration unit, Rankine cycle and PBR. Source: the authors

Incinerator and Post-Combustion chamber: The incineration unit is divided in incinerator and post-combustion chamber. Both components supply the rich CO_2 hot flue gas to a Rankine cycle and to the PBR. The incinerator can process up to 50 kg/h of MSW, while the post-combustion chamber burns liquefied petroleum gas (LPG) to assure the exiting post-combustion chamber, identified as gas5, temperature is above 900ºC. The fan supplies the preheated combustion air in a slight above stoichiometric rate (air excess, α, equal to 1.012). The fan pressure head, $P_{out,fan}$, and its flow rate are described in Eq. (1), as a function of the volumetric flow rate, $\dot{V}_{out,fan}$, based on a characteristic flow *versus* pressure curve for a centrifugal fan(14).

$$P_{out,fan} = -5 \cdot 10^{-4} \cdot \dot{V}_{out,fan}^{\,2} - 0.1989 \cdot \dot{V}_{out,fan} + 390.3 \quad (1)$$

The combustion of solid fuel, MSW, and the gaseous fuel, LPG, are modeled based on its chemical composition, shown in Table 1, with a combined incinerator and post-combustion chamber efficiency equals to 90% related to the LHV. The combustion models follows as described in the literature (15,16). The gaseous fuel combustion, LPG in this case, follows the chemical reaction described in Eq. (2), in which *MF* stands for the molar fraction for each substance, here, propane and butane. In the combustion of LPG, it is not considered any air excess, so here α_{LPG} is equal to one. The symbols *a*, *b*, *cc*, *d*, and *g* represent the number of moles for the atmospheric air, CO_2, H_2O, N_2 and O_2, respectively. The constant 3.76 multiplying N_2 is due to the hypothesis that the atmospheric air is composed of 21% of oxygen and 79% of nitrogen. For each part of oxygen 3.76 parts of nitrogen are present in the air mixture.

$$MF_{prop} \cdot C_3H_8 + MF_{but} \cdot C_4H_{10} + \alpha_{LPG} \cdot a \cdot \left(O_2 + 3.76 \cdot N_2\right) \rightarrow b \cdot CO_2 + cc \cdot H_2O + d \cdot N_2 + g \cdot O_2 \quad (2)$$

The Eq. (3) returns the mass flow rate of CO_2 generated in the powerplant, in kg/s, function of the total mass flow rate of gas, $\dot{m}_{gas}$, and the mass fraction of CO_2 in the total amount of gas.

Table 1. LPG, MSW and air composition.

LPG			MSW	
LHV (kJ/kg)	45935.7		LHV (kJ/kg)	11335.7
Molar fraction			Mass fraction	
Propane	50.0%		C	30.00%
Butane	50.0%		H	17.56%
Air Mass fraction			O	10.93%
N_2	78.81%		N	4.27%
O_2	20.96%		S	5.78%
H_2O	0.23%		Z	1.46%
			W	30.00%

$$R_{CO_2,gen} = \dot{m}_{gas} \cdot \frac{m_{CO_2}}{m_{gas}} \tag{3}$$

The properties for air and gases are calculated based on the mass fraction of each element in each stream, using the EES software properties library, except for the specific heat that is given by a polynomial model as a function of its temperature, (15).

Boiler and heat exchangers: The system central components in Figure 1comprise the heat exchanger set. The HX1 heat exchanger is the pressurized water preheater, the HX2 is the water boiler, HX3 is the vapor super-heater, HX4 is the combustion air preheater, and finally, the HX5 works as a gas cooler before the PBR to guarantee the flue gas no warmer than 40°C to avoid damaging the microalgae culture. The water vapor mass flow rate is equal to 160 kg/h, with a condensing temperature of 60°C and super-heated vapor at 250°C and 800 kPa. The condenser and HX5preheated exiting cooling water (water2 and water4, respectively) are considered as system products to be consumed by other modules of the facility, since the preheated water helps to operate their processes. Choo *et al*., 2014 (17), also shows the use potential of preheated water by a central utility building in an academic campus, as suggested in this work for condenser and HX5 products. The heat exchangers are modeled as available in the literature (18,19). The water heating process in the heat exchangers are considered a way of saving CO_2 emissions with LPG or natural gas fired heaters in facilities that require hot water. Consequently, an equivalent CO_2 conversion is done to the preheated water flows water2 and water4, as shown in Eq. (4) and Eq. (5). The mass flow rate of LPG saved in the facility with preheating water, $\dot{m}_{LPG,water}$, is given by Eq. (4), and the equivalent mass flow rate of CO_2 saved by the preheating in the systems heat exchangers is given by Eq. (5), where *MM* is the molar mass for each substance.

$$\Sigma\left(\dot{m}_{water} \cdot \Delta h_{water}\right) = \dot{m}_{LPG,water} \cdot LHV_{LPG} \tag{4}$$

$$\dot{m}_{CO_2,water} = b \cdot \frac{MM_{CO_2}}{MM_{gas}} \cdot \dot{m}_{gas,LPG,water} \tag{5}$$

Rankine Cycle: The Rankine Cycle is designed to supply 15 kW of power with a turbine under construction expected to have a low isentropic efficiency of 55%to 65%. For the Rankine water pumps it is considered an isentropic efficiency of 75%. The Rankine cycle is modeled as available in the literature (15,20).

Photobioreactors: The PBR set are built with six 10 m³ polyvinyl chloride (PVC) transparent tubular units, as shown in (21). The PBR are modeled as CO_2 consumers and microalgae biomass producers, as described in the Eq. (6) to Eq. (8) (22). In Eq. (6) and Eq. (7), $R_{CO2,cons,m^3,h}$ and $R_{bio,gen,m^3,h}$ are, respectively, the rates for CO_2 mass consumption and biomass generation per m³ of PBR (V_{PBR}) per hour of sun irradiance. The values of $R_{CO2,max}$ and $R_{bio,max}$ are adjusted based on the results of Chisti(3), considering their geometric configuration, solar irradiance for the city of Almeria, in southeast Spain, with the typical meteorological year (TMY2) data (23) and a production of 100.000 kg of biomass and consumption of 183.333 kg of CO_2 per year. The PBR model also predicts the effect of photoinhibition in the biomass production with the exponential terms for values of *I* higher than I_{max}. The values for $R_{CO2,max}$ and $R_{bio,max}$ that adjust the Chisti's work in Almeria city conditions, with this work conditions, located in the Curitiba city, in southern Brazil, are 0.3635 kg/m^3·h and 0.1983 kg/m^3·h, respectively. The Eq. (6) and Eq. (7) gives the mass flow rate of CO_2 consumed and the mass flow rate of generated biomass, both in kg/h. The Eq. (8) gives the net amount of CO_2 emitted after the PBR, calculated by the difference of CO_2 generated minus the CO_2 consumed in the biomass production. And the Eq. (9) explicit the mass flow rate of CO_2 absorbed by the biomass.

$$R_{CO_2,cons} = \left(R_{CO_2,max} \cdot I_{solar} / I_{max}\right) \cdot EXP\left(1 - I_{solar} / I_{max}\right) \cdot V_{PBR} \tag{6}$$

$$\dot{m}_{bio,gen} = \left(R_{bio,max} \cdot I_{solar} / I_{max}\right) \cdot EXP\left(1 - I_{solar} / I_{max}\right) \cdot V_{PBR} \tag{7}$$

$$R_{CO_2,emit} = R_{CO_2,gen} - R_{CO_2,cons} \tag{8}$$

$$\dot{m}_{CO_2,bio} = R_{CO_2,cons} \tag{9}$$

Each PBR are constructed with 14 individual sections, allowing distinct microalgae growth in a single equipment. The PBR dilution rate is equal 0.384/day with a concentration of 2.5% of biodigester effluent dissolved in the feed water.

CO_2balance analysis: The amount of CO_2 generated in the system depends only on the amount of fuel being consumed. Some amount of CO_2 is actually absorbed by the PBR in the biomass production and will lead to a better value of CO_2 emitted for kWh of power supplied by the Rankine Cycle. However, the system products may be considered a way of saving or compensating some CO_2 emissions, since less fuel will be required to be used or because some fuel may be replaced. The savings in CO_2emissions lead by the preheated water was already described in Eq. (5). If the microalgae biomass produced in the PBR be directed only to fuel production, some other kind of fuel, e.g., fossil fuels, may be replaced, leading to a better net value of CO_2 emitted by electric kWh produced in this integrated system. The amount of CO_2 related for each kWh of

electricity produced, or the Emission Factors, *EF*, in g_{CO2}/kWh, is given by Eq. (10).This factor reflects the total yearly production of biomass and the yearlong emission and absorption of CO_2over the 3843 hours of operation in the year. Only a fraction of the biomass production is considered in this CO_2compensation, and this conversion of biomass to oil is given by the term *BtO*. It is considered that 50% of the carbon in the biomass will be compensated as carbon on oil fuels.

$$EF = \sum \frac{\left(R_{CO_2,emit} - \dot{m}_{CO_2,water} - BtO \cdot \dot{m}_{CO_2,bio}\right)}{\left(Wturb \cdot 3843\,h\right)} \tag{10}$$

Exergoeconomic Model

In this work, the exergoeconomic analysis is based on Bejan *et al*. (12) in which a cost balance is weighted on the exergy balance for each equipment and for the overall system. The exergy represents the theoretical maximum work possible to be extracted from a system in a specific environment. The exergy for an open system is described in Eq. (11), for a system with enthalpy and entropy *h*, and *s*, an environment with states h_0, s_0 and T_0, and chemical exergy e_{ch}. The cost balance, in Eq. (12), shows that the cost rate of a product ($\dot{C}_P$, US$/h) must be equal to the sum of the equipment fuel cost rate, $\dot{C}_F$, and the non-exergetic costs rate ($\dot{Z}$, US$/h). All the exergetic related cost rates are defined as the product of its average cost per unit of exergy (*c*, US$/kJ), and its exergy rate ($\dot{E}$, kJ/h), as shown in Eq. (13) for any product. The total non-exergetic costs rate of an equipment $\dot{Z}_k$, is given by the sum of capital investment (*CI*) and operation and maintenance (*OM*) costs, in Eq. (14). The value $\dot{E}_D$, in Eq. (15), is the rate of exergy destruction and is credited with the cost of the equipment fuel ($c_{F,k}$). Each average cost per unit of exergy, *c*, is determined based on the electricity, water and other consumable costs or based on auxiliary relations given for each equipment in Bejan *et al*. (12), and its cost balances.

$$e = \left(h - h_0\right) - T_0 \cdot \left(s - s_0\right) + e_{ch} \tag{11}$$

$$\dot{C}_{P,k} = \dot{C}_{F,k} + \dot{Z}_k \tag{12}$$

$$\dot{C}_P = c_P \cdot \dot{E}_P \tag{13}$$

$$\dot{Z}_k = \dot{Z}_k^{CI} + \dot{Z}_k^{OM} \tag{14}$$

$$\dot{C}_{D,k} = c_{F,k} \cdot \dot{E}_{D,k} \tag{15}$$

In the cost balance, in Eq. (16), all the entering cost rates must be equal to the exiting cost rates. For most equipment the products average cost per unit of exergy ($c_{P,k}$) are defined by this cost balance. The cost rate for investment capital ($\dot{Z}_{CI}$), in Eq. (17), is defined based on the equipment expected life span in hours and is calculated on a levelized annual current cost using the constant escalation levelization factor (CELF) (24). The operation and maintenance (OM) costs are levelized for an expected10-year equipment life span, considering an annual wage of 7500 US$ (5.50BR$ = 1 US$) for one employee and 5% of the total CI invested per year to maintenance. The value of $\dot{Z}_{OM}$ is proportionally calculated for each equipment based on the total facility CI, as shown in the Eq. (18).

$$\underbrace{\dot{C}_{i,k} + \dot{Z}_k}_{\substack{entering \\ cost}} = \underbrace{\dot{C}_{e,k} + \dot{C}_{w,k} + \dot{C}_{q,k} + \dot{C}_{D,k}}_{\substack{exiting \\ cost}} \tag{16}$$

$$\dot{Z}_{CI,k} = CI_k \,/\, hours$$

$$\dot{Z}_{OM,k} = \left(\left(\left(Annual\ wage\right) \cdot \frac{CELF}{h_{year}} \right) + \left(CI_{total} \cdot \frac{Maintenance}{h_{year}} \right) \right) \cdot \frac{CI_k}{CI_{total}} \tag{17}$$

Additional equations are required to complete the exergoeconomic analysis. The definition of fuel and product for each component ought to be implemented, as well as to define the average cost per unit of exergy to the fuel, $c_{f,k}$, and to the product, $c_{p,k}$. These additional equations are found in the reference literature (12,16). The exergoeconomic analysis is based on a set of metrics such as exergetic efficiency (ε_k), exergoeconomic factor (f_k), relative cost difference (r_k), cost rate of exergy destruction ($\dot{C}_{D,k}$), and its sums with the non exergetic costs ($\dot{Z}_k$), $\dot{Z}_k\dot{C}_{D,k}$, for each component.

The exergetic efficiency, ε_k, in Eq. (19), shows how the equipment converts its fuel exergy rate into product exergy rate. The exergy destruction ratio, y_D, in Eq. (20), shows how much each equipment destroys of the system total fuel exergy rate. For each equipment the relative cost difference, r_k, in Eq. (21), shows how much of its product average cost is modified by its average fuel costs and non exergetic costs. The relative cost difference is useful for isolated equipment optimization and its minimization delivers the minimum average product cost compared to a fixed fuel average cost. To proceed this optimization it is required to set $\dot{E}_{P,k}$ and $c_{F,k}$ as constant to mathematically isolate the equipment from the system, as made explicit in Eq. (22) and Eq. (23), respectively. The exergoeconomic factor, f_k, in Eq. (24), compares the non-exergetic cost rate to the cost rate of exergy destruction. Values higher than 50% for f_k implies the equipment would be more cost-effective if its total price could be reduced, even with a decrease in its efficiency. On the other side, values for f_k lower than 50% suggests an improvement in efficiency would lead to a better cost-effective equipment, even with an increase in its CI or OM costs. The priorities to investigate the system components in the exergoeconomic analysis is determined by the value $\dot{Z}_k\dot{C}_{D,k}$, as shown in Eq. (25). The value $\dot{Z}_k\dot{C}_{D,k}$ is given by the sum of cast rate with

exergy destruction and the total rate of non-exergetic costs. The higher the value of $\dot{Z}_k\dot{C}_{D,k}$ for a given equipment k, the higher is the priority to analyze it.

$$\varepsilon_k = (100\%)\cdot \dot{E}_{P,k} \big/ \dot{E}_{F,k}$$
$$y_{D,k} = (100\%)\cdot \dot{E}_{D,k} \big/ \dot{E}_{F,total} \quad (18)$$

$$r_k = \frac{c_{P,k} - c_{F,k}}{c_{F,k}} = \frac{1-\varepsilon_k}{\varepsilon_k} + \frac{\dot{Z}_k}{c_{F,k}\cdot \dot{E}_{P,k}} \quad (19)$$

$$\dot{E}_{P,k} = constant \quad (20)$$

$$c_{F,k} = constant \quad (21)$$

$$f_k = (100\%)\cdot (\dot{Z}_k) \big/ \left(\dot{Z}_k + c_{F,k}\cdot \dot{E}_{D,k}\right) \quad (22)$$

$$\dot{Z}_k\dot{C}_{D,k} = \dot{C}_{D,k} + \dot{Z}_k \quad (23)$$

With the objective of optimize the components for the minimum average product cost, the exergoeconomic analysis suggests prioritizing the components as follows:

First analyze the components with larger value of $\dot{Z}_k\dot{C}_{D,k}$. 2) Among those, analyze the ones with larger relative cost difference r_k. 3) Verify the exergoeconomic factor, f_k, if the component requires better efficiency or lower CI and OM costs. 4) Investigate the components with low exergetic efficiency, ε_k, and high exergy destruction ratio (y_D) (12). The components CI variation must be estimated depending on its key variables. The CI prediction equations may be modified to better adapt to this work. In these equations, each term B_k is a constant used to convert the values in Brazilian Real to USDollars (5.50BR$ for 1 US$) and to adjust the values by inflation in each currency as needed, up to the period ofJanuary 2022. The B_k values are shown in Table 2.

Table 2. Values for B_k constant in CI predictions for each equipment Eq. (26) to Eq. (28).

B_{HX1}=862.70	B_{HX5}=832.52	B_{turb}=38400.28
B_{HX2}=257265.45	B_{fan}=9337308.73	B_{cond}=25409.10
B_{HX3}=862.70	B_{inc}=11601.71	B_{pump}=1495.67
B_{HX4}=862.70	$B_{poscomb}$=113.43	B_{cycl}=12704.55

The heat transfer area is the parameter used to predict the heat exchanger CI variation, as shown in Eq. (26). Initially all heat exchangers are considered with a reference area of 10 m² (25, 26).

$$CI_{HX,k} = B_k \cdot (10 + A_{HX,k}{}^{0,8}), \ \mathrm{k} = [1,3,4,5] \quad (26)$$

The CI predictionto the incinerator is based on its mass flow rate incineration capacity, modeled as a gasification chamber, as shown in Eq (27).

$$CI_{inc} = B_k \cdot \dot{m}_{MSW}{}^{0.67} \quad (27)$$

The turbine CI is modeled as a function of its power output ($\dot{W}_{turb}$), inlet vapor temperature (T_{vap4}) and isentropic efficiency (η_{turb}), as shown in Eq. (28)(27). No CI variation is implemented to the cyclone, and its CI is equal to B_{cycl}. And last of all, in Eq. (29), the PBR CI variation is determined as a function of its materials and construction prices. The equations to CI prediction of heat exchanger HX2, post-combustion chamber, condenser, pumps and fans are shown in Galante, 2019 (16).

$$CI_{turb} = B_k \cdot \dot{W}_{turb}{}^{0.7} \times \left(1 + \left(\frac{0.05}{1-\eta_{turb}}\right)^3\right) \cdot \left(1 + 5\cdot \exp\left(\frac{T_{vap} + 273.15 - 866}{10.42}\right)\right) \quad (28)$$

$$CI_{PBR} = (0.5 + 0.5\cdot n_{PBR})\cdot 1399.4 + n_{PBR}\cdot 637.7 \quad (29)$$

The cost of consumables as water and electricity are given in Table 3, as well as the incineration service and the reference microalgae biomass cost. The incineration operated by the system must be considered as a service performed to the university campus that has an economic return to the system, referred as a subsidy, as shown in Eq. (30), where C_{inc} is the cost of the third-party incineration services US$/kg, and $FC_{subsidy}$ is a fraction of this incineration cost. The subsidy is considered as a system cash inflow, as shown in Eq. (31). Since the system products are going to be directed to other modules in the same facility no profit will be added to its selling prices. If the products are to be sold with its product cost as selling price, no profitability would be expected in a finite payback period. So, in the baseline model, the subsidy, $FC_{subsidy}$, is always equal to

20% as it is needed to the system economic feasibility. Initially no cost is attributed to the MSW as a fuel. However, some analysis may consider a fuel cost, also in the form of a fraction of the incineration cost, FC_{inc}, in Eq. (32), where c_{MSW} is defined based on the cost of incineration per kg, C_{inc}, in Eq. (33). Considering the analysis of MSW fuel cost, the FC_{inc} value varies from 0% to 1.75%. At the time of this work the university pays 0.66 US$/kg to a third-party company to incinerate some sorts of residues.

Table 2. Cost of consumables and residues incineration

Grid electricity price	0.18 US$/kWh
LPG Price	1.89 US$/kg
Water price	2.32 US$/m³
Effluent price	0 US$/kg
MSW price	0 US$/kg
Third-party incineration services	0.67 US$/kg
Reference biomass (3)	0.63 S$/kg

The biomass reference price follows the experimental data in Chisti, 2007(3), which value is adjusted by the US Dollar inflation (28) from January 2007 to January 2022, resulting in 0.622 US$/kg of biomass. The biomass cost is defined by its exergoeconomic cost rate divided by its production mass flow rate, as shown in Eq. (34). In the situations where the cost of electricity generated in the system is higher than the one supplied by the grid, the variable $\Delta C_{electric}$ is considered to discuss the electricity prices difference in the operating system, in Eq. (35). Another useful variable to analyze the system is the payback period, *PP*, defined as follows in Eq. (36), as a function of the total capital investment in the system and the hourly cash flow, in Eq. (37), along the plant lifetime.

$$\dot{C}_{subsidy} = \left(C_{inc} \cdot FC_{subsidy} \right) \cdot \dot{E}_{MSW} \Big/ LHV_{MSW} \tag{30}$$

$$Cash_{in} = \dot{C}_{subsidy} + \dot{C}_{bio} + \dot{C}_{W,turb} + \dot{C}_{bio} + \dot{C}_{water2} + \dot{C}_{water4} \tag{31}$$

$$Cash_{out} = \left(c_{MSW} \cdot FC_{inc} \right) \cdot \dot{E}_{MSW} + \dot{C}_{LPG} + \dot{C}_{elect} + \dot{Z}_{OM,total} \tag{32}$$

$$c_{MSW} = FC_{inc} \cdot C_{inc} \Big/ LHV_{MSW} \tag{33}$$

$$C_{bio} = \dot{C}_{bio} \Big/ \dot{m}_{bio} \tag{34}$$

$$\Delta C_{electric} = \left(c_{P,turb} - c_{elect} \right) \cdot \dot{E}_{P,turb} \tag{35}$$

$$PP = \left(CI_{tot} \right) \Big/ \left(h_{year} \cdot \left(Cash\ Flow \right) \right) \tag{36}$$

$$Cash\ Flow = Cash_{in} - Cash_{out} \tag{37}$$

RESULTS AND DISCUSSION

The results for each point in the baseline model system (Figure 1) are shown in Table 4. It shows temperature, pressure, mass flow rate, exergy rate, average cost per unit of exergy and cost rate for each system point. These results come from the solution of energy, exergy, and cost balances on each equipment, as described in the previous section. With Eq. (19) to (25) it is possible to obtain the exergoeconomic results of Table 5. The baseline model and the individual equipment simulations are performed with a solar irradiance of 390 W/m², an averaged value from the 3843 hours of operation per year only for solar irradiance higher than 50 W/m². The data in Table 5follows the recommendations for prioritizing the components in exergoeconomic analysis, organizing then by the higher $\dot{Z}_k \dot{C}_{D,k}$ values. By these results the equipment with the higher priority to be analyzed is the turbine. The results also show the low exergoeconomic efficiency of some components. The HX4, HX5 and condenser have low ε_E because their products are the cooling water or preheated air streams, which are in lower exergetic levels with low temperatures. The fan receives high quality exergy in form of electricity and its product has low exergy level, with low temperature difference and low-pressure flow. The PBR, like other solar powered components, has low efficiency due the high-quality exergy that it receives from the sun incidence, generating a small amount of high exergy product in the form of biomass. This is also the reason the PBR has the second highest exergy destruction rate, y_D. The highest y_D is a usual result for an incinerator, since it receives and burn a high-density chemical exergy fuel resulting in a stream of heated flue gas. The combustion process is commonly associated with high exergy destruction rate (12). The Figure 2 shows the impact of subsidy for the incineration services to the system payback. With $FC_{subsidy}$ as low as 7% the system would have a payback almost as high as 10 years. For all conditions in this work, it is considered a 20% $FC_{subsidy}$ as a payment for the incineration services, decreasing the baseline payback time for 3.9 years. Following the exergoeconomic priorities, the turbine is the first component to be analyzed. The Figure 3 shows the turbine optimization via r_{turb} minimization, with results for inlet vapor temperature ranging from 250°C to 570°C and isentropic efficiency, η_{turb}, starting in 55% to 65%, while keeping the required *r* minimization restrictions of Eq. (22) and Eq. (23). The minimum r_{turb}

values are found around 520°C for all η_{turb} analyzed. This behavior is due the turbine investment capital prediction following the Eq. (28), which shows no significant variation for inlet vapor temperature lower than 460°C.

Table 3. Base model system results for each point of Figure 1

Point	T (°C)	ṁ (kg/h)	Ė (kJ/h)	c (US$/kJ)
Air1	25.00	476.34	23309.17	0.00E+00
Air2	125.00	476.34	30051.36	1.46E-05
Fan_{in}	125.00	476.34	30051.36	1.46E-05
Fan_{out}	125.45	476.34	30106.77	2.37E-05
MSW	25.00	47.82	849731.36	0.00E+00
LPG	25.00	1.39	67684.96	4.12E-05
Gas3	843.87	502.34	375386.68	6.38E-06
Gas5	900.00	525.00	422389.10	1.39E-05
Gas6	860.96	525.00	400790.31	1.39E-05
Gas7	376.22	525.00	175806.88	1.39E-05
Gas8	283.07	525.00	145027.71	1.39E-05
Gas9	207.81	525.00	124579.08	1.39E-05
Gas10	40.00	449.46	63351.71	1.39E-05
Water10	40.00	75.54	304.21	0.00E+00
Gas11	39.72	449.32	63345.06	1.61E-05
Gas12	25.00	452.64	55901.94	0.00E+00
Vap1	60.00	160.00	1387.28	5.15E-05
Vap2	150.00	160.00	14074.62	4.65E-05
Vap3	170.44	160.00	125923.03	3.56E-05
Vap4	250.00	160.00	136912.81	3.61E-05
Vap5	59.90	160.00	40684.04	3.61E-05
Liq6	59.90	160.00	1255.90	3.61E-05
Water1	25.00	4497.48	11243.69	9.36E-04
Water2	45.00	4497.48	23324.26	5.24E-04
Water3	25.00	1250.77	3126.92	9.36E-04
Water4	45.00	1250.77	6486.58	6.05E-04
Biomass	25.00	8.77	201815.36	1.70E-05
Effluent	25.00	23929.49	215365.38	0.00E+00
Ash	39.72	0.70	1.25	0.00E+00

Table 4. Exergoeconomic main results The five highest values are highlighted for $\dot{Z}_k\dot{C}_{D,k}$, r_k, f_k and y_D, and the five lowest ones for ε_k.

Equip.	$\dot{Z}_k\dot{C}_{D,k}$	r_k	f_k	ε_k	y_D
	(US$/h)	(-)	(%)	(%)	(%)
Turb	4.35	2.17	66.29	57.72	2.77
PBR	3.00	9.19	80.29	32.96	24.17
HX2	2.27	1.46	30.79	49.71	7.71
Inc	2.10	7.21	81.37	42.73	34.39
Cond	1.27	2.91	22.16	30.64	1.86
Poscomb	1.25	0.19	52.48	95.04	3.46
HX5	0.95	20.44	15.79	5.49	3.93
HX1	0.41	2.31	38.21	41.22	1.23
HX4	0.35	3.69	44.94	32.97	0.93
HX3	0.30	1.98	51.32	50.88	0.72
Fan	0.27	96.31	96.90	25.11	0.01
Cyclone	0.14	0.16	99.94	99.99	0.00
Pump	0.02	2.91	90.10	77.62	0.00

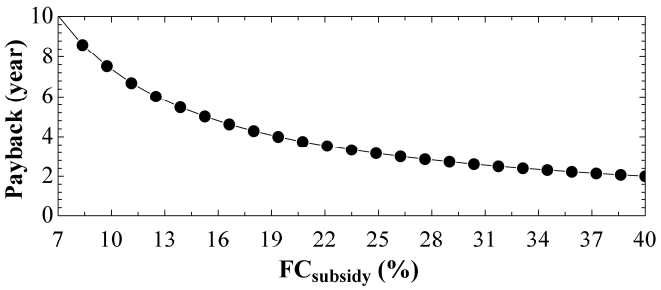

Figure 2. System payback versus the cost fraction of third-party incineration services this cost fraction is attributed as a system positive remuneration paid incineration services

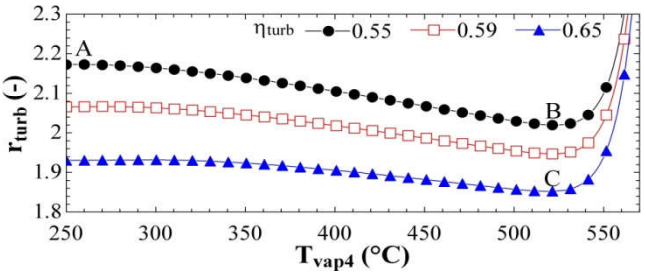

Figure 3. Turbine optimization via r_{turb} minimization as a function of its vapor inlet temperature, T_{vap4}, and isentropic efficiency, η_{turb}.

Table 5. Baseline system as Turb A, and system results for optimized turbine, with conditions B and C, shown in Figure 3

Modified Parameters	Turb. A	Turb. B	Turb. C
η_{turb}	0.55	0.55	0.65
T_{vap4} (□C)	250.00	523.40	519.3
$\dot{m}_{vap}$ (kg/h)	160.00	110.30	93.88
$C_{W,turb}$ (US$/kWh)	0.41	0.38	0.40
C_{bio} (US$/kg)	0.39	0.39	0.40
$\Delta C_{water1,2}$ (US$/m³)	0.38	0.45	0.47
$\Delta C_{water3,4}$ (US$/m³)	0.80	0.69	0.68
$\Delta C_{electric}$ (US$/kWh)	0.23	0.20	0.22
r_{turb} (-)	2.17	2.11	2.14
f_{turb} (%)	66.29	73.40	73.68
Payback (year)	3.89	3.69	3.51

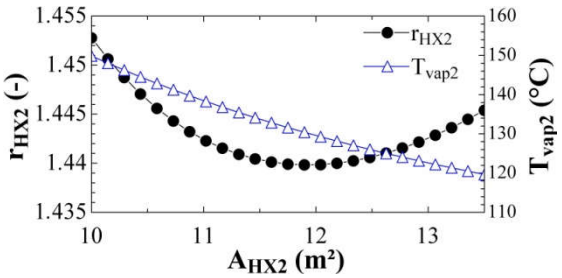

Figure 4. r_{HX2} minimization and T_{vap2} as a function of HX2 heat transfer area

The entire system operating with the parameters that results in minimum r_{turb}, are analyzed with no restrictions from Eq. (22) and Eq. (23). The results for the system operating in the optimum turbine conditions of Figure 3, in the points A, B and C, are shown in Table 6. The prices of all the system products (electricity, biomass, hot cooling water water4 and water2) fluctuate due to the new conditions imposed by the modified parameters and the new cost balance in the system streams. For instance, the cost for each m³ of hot cooling water water4, C_{water4} (US$/m³), is decreased due to the higher water mass flow rate required to cool the warmer hot flue gas, since the vapor mass flow rate was decreased in the turbine, and a higher amount of heat was left in the hot flue gas. The turbine optimization by itself resulted in lower difference in electricity price with the grid electricity, $\Delta C_{electric}$, from 0.23 to 0.20 and 0.22 US$/kWh, and a reduction in the payback period from 3.89 to 3.69 and 3.51 years, in the turbine cases A, B and C, respectively. Because the last step of optimization, Turb.C, depends on a more optimistic isentropic efficiency to the turbine, the case Turb. B is taken as the optimized turbine option. Although the turbine exergetic factor originally suggested a reduction in the turbine costs (f_{turb} higher than 50%), the r_{turb} minimization resulted in an even costlier equipment, and no more efficient than the initial condition. In this case, the payback analysis supports the decision for accepting the optimized turbine in the system.

The PBR is the second equipment to be analyzed by the exergoeconomic analysis priorities, as indicated in Table 5. This is a modular equipment, and its productivity and price follow a linear proportion to its volume and number of units, as shown in Eq. (7) and Eq. (29). However, the exergoeconomic PBR fuels, i.e., flue gas, solar incidence and biodigester effluent, are cheap and abundant in this plant. So, the increase in PBR units leads to a cheaper biomass production, C_{bio} in US$/kg, but, on the other hand, a constant increment in payback time. Since the additional cost in PBR do not lead to better production per volume it is not possible to optimize this component with the exergoeconomic analysis as it is modelled. Consequently, the final optimized system will remain with 6 PBR units, based on the currently actual plant. The component HX2 i.e., Rankine evaporator, is the third component to be optimized (Table 5), and its optimization is shown in Figure 4. Its already low value of relative cost, r_{HX2}, is minimized to its lower value with a heat exchanger area of 12.63 m² and an inlet water temperature, T_{vap2}, of 124.9°C. With the unrestricted system operating with the HX2 optmized parameters the system payback was increased in 12.5% and had a slightly increase in the electricity cost difference, $\Delta C_{electric}$. This additional payback period happaned due the reduction in vapor flow rate and consequently reduction in the turbine power. Therefore, the optmized HX2 will not be applied in the final system optmization.

The incinerator is the next optimization priority as shown in Table 5, and its results are shown in Figure 5. Its optimization is performed with the variation of preheated air temperature, T_{air2}, and the MSW cost. Its cost is attributed to a fraction of the third-party incineration service cost, as shown in Eq. (33). The incinerator exergoeconomic fuel is both the MSW and preheated air. The values for r_{inc} have a minimum for each FC_{inc}, and each minimum r_{inc} has an equivalent T_{air2}. The optimum values of T_{air2} ranges from 240°C for FC_{inc} equal to 0.0%, and 370°C for FC_{inc} equal to 1.75%. It shows the high dependency of fuel cost to optimize the incinerator, what could become a struggle with high diversity of MSW on a large scale scenario. The value of FC_{inc}equal to1.75% is the chosen condition to the optimized incinerator in following analysis.

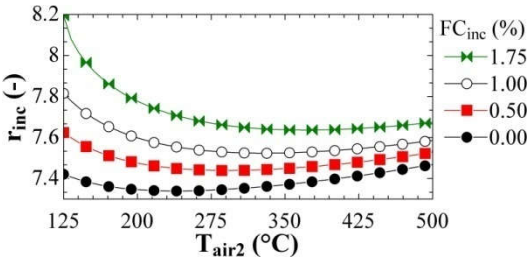

Figure 5 – Incinerator rinc minimization as a function of preheated air intake, T_{air2}, and the cost attributed to the MSW as a fraction of the third-party incineration cost

Table 6. Results for the baseline system: Case A: system with no optimized incinerator and FC_{inc} fuel cost equal to 0%. Case B: optimized incinerator and FC_{inc} fuel cost equal to 1.75%. Case C: optimized incinerator and FC_{inc} fuel cost equal to 0%. Case D: optimized incinerator and FC_{inc} fuel cost equal to 1.75%. The incinerator optimization occurs for T_{air2} equal 370°C

Modified parameters	Baseline, A	Case B	Case C	Case D
FC_{inc} (%)	0.0	1.75	0.0	1.75
$\dot{C}_{MSW}$ (US$/ton)	0.0	11.72	0.0	11.72
T_{air2} (°C)	125.0	125.0	370.0	370.0
$\dot{m}_{LPG}$ (kg/h)	1.39	1.39	0.0	0.0
$C_{W,turb}$ (US$/kWh)	0.41	0.44	0.33	0.36
C_{bio} (US$/kg)	0.39	0.41	0.34	0.36
$\Delta C_{water1,2}$ (US$/m³)	0.38	0.42	0.26	0.31
$\Delta C_{water3,4}$ (US$/m³)	0.80	0.90	0.58	0.71
$\Delta C_{electric}$ (US$/kWh)	0.23	0.26	0.15	0.18
r_{inc} (-)	7.21	3.84	3.74	2.43
f_{inc} (%)	81.37	65.02	74.30	60.57
Payback (year)	3.89	4.05	3.39	3.52

All the system products have increased prices with MSW going from FC_{inc} equals 0% to 1,75%, comparing Case A to Case B in Table 7. However, when applied the optimal T_{air2} temperature of 370°C in the HX4 air preheater (Case D), the incinerator works in its optimized condition. In this case, the system products prices are lower even when compared with the baseline condition. The reason for such cost reduction lays in the exiting gas temperature. With T_{air2} equal to 370°C, the flue gas temperature, T_{gas3}, leaving the incinerator, is equal to 1015°C. So, in the condition were T_{gas3} is higher than 900°C, no LPG burning is needed, and a cost rate of 2.41 US$/h with LPG (Table 4) is reduced. This explains the payback of Case D even lower than the one in baseline Case A. The case D has the nearest f_{inc} from 50%. Considering the exergoeconomic factor, an expensive incinerator has its costs better justified if processing an expensive fuel. Consequently, the Case D is the better balanced one from an exergoeconomic point of view.

The condenser is the next exergoeconomic priority in Table 5. Its optimization leads to an increase in the payback period, mostly because it requires a lower vapor mass flow rate, what reduces directly the power supplied by the turbine. The optimized condenser will not be included in the optimized system. The optimized post-combustion chamber will also not be included in the optimized system. Within the constraints of Eq. (22) and Eq. (23), the $r_{poscomb}$ minimization occurred to T_{gas5} equal to 1317°C, what requires an impeditive use of LPG, going from 1.4 kg/h to 8.0 kg/h and increasing all the downstream costs in the system. In this condition, there would be a negative cash flow, and no possible payback. The heat exchanger HX5 is the component responsible for cooling the flue gas to be sent to the PBR. It is optimized with no significant impact over the system payback, as shown in Table 8. However, its optimization resulted in warm cooling water in a higher temperature, from 45°C to 88.7°C. The higher water outlet temperature led to a reduction in water mass flow rate, increasing the preheated water, *water 4*, price from 3.12 US$/m³ to 4.83 US$/m³. However, when analyzed the average price per unit of exergy, in US$/kJ, its optimization resulted in a price 2.9 times lower than the baseline.

The component HX1 optimization goes in the opposite direction of the turbine optimization requirements and will not be included in the overall system optimization. The heat exchanger HX4 was optimized, but lead to an 11% increase in payback period, and was not implemented in the optimized system. The heat exchanger HX3 shown no condition of optimization within the system conditions. The complete system optimization is performed with the optimized version of the turbine, incinerator and HX5. The results for the sequential components optimization are shown in Table 9. This simulation is performed considering the FC_{inc} equal to 1.75% in Eq. (32) for the MSW fuel price, and average solar irradiance equals 390 W/m². It starts from the baseline system, with a payback of 4.05 years. The system with the optimized turbine has a 5.9% lower payback, equal to 3.81 year. The optimization of turbine and incinerator together leads to a payback equal 3.37 years. The optimized HX5 results in no significant payback variation, however, it leads to warm cooling water, *water4*, in a higher temperature (45°C to 88.7°C) and lower price in US$/kJ. The electricity price varies from 0.44 US$/kWh (baseline) to 0.34 US$/kWh (complete optimization), respectively 145% and 89%more expensive than the electricity supplied by the grid. Comparing the two streams of preheated water supplied by the system cooling water (*water 2* and *water 4*) and comparing them with a 100% efficiency LPG water heater, the condenser supplies water at 45°C with a cost 8.9 times lower and the HX5 supplies water at 88.7°C with a cost 5.9 times lower. These preheated water streams are aimed to be consumed by the neighboring facilities. A similar simulation, performed with FC_{inc} equal to 0%, removing the MSW fuel cost, results in a payback that varies from baseline 3.89 years, to 3.69 with optimized turbine, to 3.26 adding the optimized incinerator and 3.26 adding the optimized HX5. A final payback value 3.2% lower than the case with FC_{inc} equal to 1.75%. The electricity price varies from 0.41 US$/kWh to 0.30 US$/kWh, respectively 127% and 67% more expensive than the electricity supplied by the grid. The PBR behavior is linked with the solar irradiance, although the biological activities are flattened in the higher incidence hours due to the photoinhibition modeled in the exponential term in Eq. (6) and (7). A steady amount of CO_2 is generated by the incinerator and post-combustion chamber, and some amount of this CO_2 is captured by the microalgae culture, to produce the biomass.

Table 7. Results for the baseline system and for the system with optimized HX5 heat exchanger

Modified Parameters	Baseline	Opt. HX5
A_{HX5} (m²)	10.0	12.94
T_{water4} (°C)	45.0	88.75
$C_{W,turb}$ (US$/kWh)	0.41	0.41
C_{bio} (US$/kg)	0.39	0.39
$\Delta C_{water1,2}$ (US$/m³)	0.38	0.38
$\Delta C_{water3,4}$ (US$/m³)	0.80	2.53
$C_{subsidy}$ (US$/kWh)	0.23	0.23
r_{HX5} (-)	20.44	6.42
f_{HX5} (%)	15.79	18.44
Payback (year)	3.89	3.89

Table 8. Results for the consecutive components optimization starting from baseline system until all three optimized components. This scenario has the MSW costing as much as FC_{inc} equal to 1.75%, and average solar irradiance equals 390 W/m²

FC_{inc} = 1.75%	Baseline	+Turb	+Inc	+HX5
$C_{W,turb}$ (US$/kWh)	0.44	0.40	0.34	0.34
c_{bio} (US$/kJ)	0.41	0.41	0.36	0.36
$\Delta C_{water1,2}$ (US$/m³)	0.42	0.50	0.36	0.36
$\Delta C_{water3,4}$ (US$/m³)	0.90	0.79	0.53	1.67
$\Delta C_{electric}$ (US$/kWh)	0.26	0.22	0.15	0.15
Cash flow (US$/h)	10.23	10.75	12.28	12.29
CI_{total} (10^3 US$)	159.29	157.47	158.85	158.99
Payback (year)	4.05	3.81	3.37	3.37
r_{turb} (-)	2.01	1.94	2.56	2.56
f_{turb} (%)	63.63	71.08	78.10	78.10
r_{inc} (-)	3.84	3.76	2.43	2.43
f_{inc} (%)	65.02	64.25	60.52	60.52
r_{HX5} (-)	20.00	17.16	19.39	6.04
f_{HX5} (%)	13.94	10.16	17.78	20.55

The year-long simulation is performed for all 3843 hours with solar irradiance higher than 0.05 kW/m² for the TMY2 data of Curitiba. The Table 10shows the results for the year-long simulation, with the average biomass product price, the amount of biomass produced, the amount of CO_2 generated by the system, and the amount captured and finally emitted in the atmosphere in four different scenarios: baseline system with FC_{inc} equals 0% and equals 1.75% as MSW fuel cost, and optimized system with FC_{inc} equals 0% and equals 1.75% as MSW fuel cost. Compared with the inflation adjusted value of Chisti, 2007 (3), equal to 0.92 US$/kg of biomass, the most expensive price in the baseline system is 50% cheaper than the reference, and the optimized results are 55% and 58% cheaper, with prices shown in Table 10. The optimized system has a lower CO_2 generation since it has no need of burning additional LPG, and it has a direct impact in the CO_2 emission factor, *EF*, results. The optimized *EF* results are comparable to biomass fired energy systems (11). The values for *EF* are highly sensitive to the amount of carbon considered going from biomass to oil, *BtO*, as shown in Table 11. With no compensation from the biomass production, the amount of CO_2 released for kWh can reach values higher than 750 g_{CO2}/kWh. On the other hand, values of BtO of 80% as described in the literature can lead to *EF* as low as 22.3 g_{CO2}/kWh, among the cleanest energy sources (2–5,11).

Table 9. Annual simulation results of biomass production and generated, consumed, and emitted CO2 for the baseline system and optimized system, with FC_{inc} equal 0% and 1.75% for the MSW fuel cost

	Baseline	Optimized	Optimized
FC_{inc}	1.75%	1.75%	0%
C_{bio} (US$/kg)	0.46	0.41	0.39
$\dot{m}_{bio}$ (kg/year)	29563	29563	29563
$\dot{m}_{CO2,gen}$ (kg/year)	218090	211288	211288
$\dot{m}_{CO2,capt}$ (kg/year)	54201	54201	54201
$\dot{m}_{CO2,emit}$ (kg/year)	163872	157074	157074
Wturb (kWh/year)	59259	59259	59259
EF (g_{CO2}/kWh)	411.4	296.7	296.7

Table 10. Emission Factor values varying with the biomass-to-oil conversion yield.

BtO (%)	0	20	40	50	60	80
EF (g_{CO2}/kWh)	754.0	571.1	388.2	296.7	205.2	22.3

CONCLUSION

This work analyzed an integrated incineration power plant fired by MSW with biological flue gas filters for microalgae biomass production in the context of a university campus in southern Brazil. The biological filter is made with 6 PBR units of 10 m³ each, which absorb flue gas CO_2 and produces microalgae mainly for biodiesel production. The integrated power plant components were examined by an exergoeconomic analysis and optimization process, aiming to verify its technical and economic feasibility. The exergoeconomic analysis proposed by Bejan *et al*. (12) was effectively used in this work. Each equipment had predictions for its investment capital varying with its main project variables, allowing to perform the exergoeconomic analysis. Considering the components analyzed, 8 out of 10 were optimized. Within the 8 optimized ones, 3 components lead to a lower system payback when compared to the baseline system. The system economic feasibility required some subsidy, in this case, the system owners must receive some payment for the incineration services. With a payment of 20% of the actual third-party

incineration cost, the system has a starting payback of 4.05 years. The baseline model showed a payback varying from4.05 to 3.89 years and the optimized system showed a payback from 3.52 to 3.39 years. The electricity generated in the power plant varies from 145% to 89% more expensive than the one supplied by the grid with the baseline and optimized system, respectively. The microalgae biomass achieved a price range from 50% to58% cheaper than the reference work with the same PBR technology costing as low as 0.39 US$/kg. The other system product is preheated water to the neighboring facilities. The 45^{o}C stream of water had a cost 8.9 times lower when compared with a 100% efficiency LPG water heater, and the 88.7^{o}C water stream had a price 5.9 times lower when compared in the same conditions. With the payback results and product prices, this integrated MSW incineration power plant is technically and economically feasible, producing clean energy.

REFERENCES

(1) S. Monni, From landfilling to waste incineration: Implications on GHG emissions of different actors, International Journal of Greenhouse Gas Control. 8 (2012) 82–89. https://doi.org/10.1016/j.ijggc.2012.02.003.

(2) P. Champagne, Chapter 9 - Biomass A2 - Letcher, Trevor M., in: Future Energy, Elsevier, Oxford, 2008: pp. 151–170. http://www.sciencedirect.com/science/article/pii/B9780080548081000090 (accessed January 18, 2017).

(3) Y. Chisti, Biodiesel from microalgae, Biotechnology Advances. 25 (2007) 294–306. https://doi.org/10.1016/j.biotechadv.2007.02.001.

(4) N. Sharma, K.K. Jaiswal, V. Kumar, M.S. Vlaskin, M. Nanda, I. Rautela, M.S. Tomar, W. Ahmad, Effect of catalyst and temperature on the quality and productivity of HTL bio-oil from microalgae: A review, Renewable Energy. 174 (2021) 810–822. https://doi.org/10.1016/j.renene.2021.04.147.

(5) J.H.K. Lim, Y.Y. Gan, H.C. Ong, B.F. Lau, W.-H. Chen, C.T. Chong, T.C. Ling, J.J. Klemeš, Utilization of microalgae for bio-jet fuel production in the aviation sector: Challenges and perspective, Renewable and Sustainable Energy Reviews. 149 (2021) 111396. https://doi.org/10.1016/j.rser.2021.111396.

(6) M. Aziz, Power generation from algae employing enhanced process integration technology, Chemical Engineering Research and Design. 109 (2016) 297–306. https://doi.org/10.1016/j.cherd.2016.02.002.

(7) S.A. Razzak, S.A.M. Ali, M.M. Hossain, H. deLasa, Biological CO2 fixation with production of microalgae in wastewater – A review, Renewable and Sustainable Energy Reviews. 76 (2017) 379–390. https://doi.org/10.1016/j.rser.2017.02.038.

(8) N.F.H. Selesu, T.V. de Oliveira, D.O. Corrêa, B. Miyawaki, A.B. Mariano, J.V.C. Vargas, R.B. Vieira, Maximum microalgae biomass harvesting via flocculation in large scale photobioreactor cultivation, The Canadian Journal of Chemical Engineering. 94 (2016) 304–309. https://doi.org/10.1002/cjce.22391.

(9) A. Toledo-Cervantes, T. Morales, Á. González, R. Muñoz, R. Lebrero, Long-term photosynthetic CO2 removal from biogas and flue-gas: Exploring the potential of closed photobioreactors for high-value biomass production, Science of The Total Environment. 640–641 (2018) 1272–1278. https://doi.org/10.1016/j.scitotenv.2018.05.270.

(10) L. Moraes, G.M. Rosa, A. MorillasEspaña, L.O. Santos, M.G. Morais, E. Molina Grima, J.A.V. Costa, F.G. Acién Fernández, Engineering strategies for the enhancement of Nannochloropsisgaditana outdoor production: Influence of the CO2 flow rate on the culture performance in tubular photobioreactors, Process Biochemistry. 76 (2019) 171–177. https://doi.org/10.1016/j.procbio.2018.10.010.

(11) J. Emblemsvåg, Wind energy is not sustainable when balanced by fossil energy, Applied Energy. 305 (2022) 117748. https://doi.org/10.1016/j.apenergy.2021.117748.

(12) A. Bejan, Bejan, Moran, G. Tsatsaronis, M. Moran, M.J. Moran, Thermal Design and Optimization, John Wiley & Sons, 1996.

(13) EES: Engineering Equation Solver | F-Chart Software : Engineering Software, (n.d.). http://www.fchart.com/ees/ (accessed January 8, 2019).

(14) Y.A. Çengel, J.M. Cimbala, Fluid Mechanics: Fundamentals and Applications, McGraw-Hill Education, 2018.

(15) M.J. Moran, H.N. Shapiro, D.D. Boettner, M.B. Bailey, Fundamentals of Engineering Thermodynamics, 8th Edition, Wiley, 2014.

(16) R.M. Galante, Análise e otimização termoeconômica de sistemas de geração de energia por incineração de resíduos com filtro biológico de emissões, (2019). https://acervodigital.ufpr.br/handle/1884/65685 (accessed April 1, 2022).

(17) K. Choo, R.M. Galante, M.M. Ohadi, Energy consumption analysis of a medium-size primary data center in an academic campus, Energy and Buildings. 76 (2014) 414–421. https://doi.org/10.1016/j.enbuild.2014.02.042.

(18) Y.A. Çengel, A.J. Ghajar, Heat and Mass Transfer: Fundamentals & Applications, McGraw-Hill Education, 2015.

(19) T.L. Bergman, A.S. Lavine, F.P. Incropera, Fundamentals of Heat and Mass Transfer, 7th Edition, John Wiley & Sons, Incorporated, 2011.

(20) Y. Çengel, M. Boles, Thermodynamics: An Engineering Approach, McGraw-Hill Education, 2010.

(21) J.V.C. Vargas, A.B. Mariano, D.O. Corrêa, J.C. Ordonez, The microalgae derived hydrogen process in compact photobioreactors, International Journal of Hydrogen Energy. 39 (2014) 9588–9598. https://doi.org/10.1016/j.ijhydene.2014.04.093.

(22) M.H. Sugai, Mathematical model of tubular photobioreactors gasification column for microalgae cultivation, M.Sc. Thesis, Federal University of Parana, 2012.

(23) Weather Data | EnergyPlus, (n.d.). https://energyplus.net/weather (accessed January 7, 2019).

(24) J. Wellmann, B. Meyer-Kahlen, T. Morosuk, Exergoeconomic evaluation of a CSP plant in combination with a desalination unit, Renewable Energy. 128 (2018) 586–602. https://doi.org/10.1016/j.renene.2017.11.070.

(25) M.A. Jamil, S.M. Zubair, Design and analysis of a forward feed multi-effect mechanical vapor compression desalination system: An exergo-economic approach, Energy. 140 (2017) 1107–1120. https://doi.org/10.1016/j.energy.2017.08.053.

(26) M. Kim, D. Kim, I.J. Esfahani, S. Lee, M. Kim, C. Yoo, Performance assessment and system optimization of a combined cycle power plant (CCPP) based on exergoeconomic and exergoenvironmental analyses, Korean J. Chem. Eng. 34 (2017) 6–19. https://doi.org/10.1007/s11814-016-0276-2.

(27) P. Roosen, S. Uhlenbruck, K. Lucas, Pareto optimization of a combined cycle power system as a decision support tool for trading off investment vs. operating costs, International Journal of Thermal Sciences. 42 (2003) 553–560. https://doi.org/10.1016/S1290-0729(03)00021-8.

(28) Consumer Price Index Data from 1913 to 2020, US Inflation Calculator. (2008). https://www.usinflationcalculator.com/inflation/consumer-price-index-and-annual-percent-changes-from-1913-to-2008/ (accessed April 26, 2020).

****